BJP British Journal of Pharmacology

DOI:10.1111/bph.12871
www.brjpharmacol.org

RESEARCH PAPER

Autocrine secretion of 15d-PGJ_2 mediates simvastatin-induced apoptotic burst in human metastatic melanoma cells

Correspondence
Martin Hohenegger, Institute of Pharmacology, Center of Physiology and Pharmacology, Comprehensive Cancer Center, Medical University of Vienna, Waehringerstrasse 13A, A-1090 Vienna, Austria. E-mail: martin.hohenegger@meduniwien.ac.at

Received
6 November 2013
Revised
14 July 2014
Accepted
29 July 2014

Christine Wasinger[1], Martin Künzl[1], Christoph Minichsdorfer[2], Christoph Höller[3], Maria Zellner[4] and Martin Hohenegger[1]

Institutes of [1]Pharmacology and [4]Physiology, Center of Physiology and Pharmacology, and Departments of [2]Internal Medicine I and [3]Dermatology, Medical University of Vienna, Vienna, Austria

BACKGROUND AND PURPOSE

Despite new therapeutic approaches, metastatic melanomas still have a poor prognosis. Statins reduce low-density lipoprotein cholesterol and exert anti-inflammatory and anti-proliferative actions. We have recently shown that simvastatin triggers an apoptotic burst in human metastatic melanoma cells by the synthesis of an autocrine factor.

EXPERIMENTAL APPROACH

The current *in vitro* study was performed in human metastatic melanoma cell lines (A375, 518a2) and primary human melanocytes and melanoma cells. The secretome of simvastatin-stressed cells was analysed with two-dimensional difference gel electrophoresis and MS. The signalling pathways involved were analysed at the protein and mRNA level using pharmacological approaches and siRNA technology.

KEY RESULTS

Simvastatin was shown to activate a stress cascade, leading to the synthesis of 15-deoxy-12,14-PGJ_2 (15d-PGJ_2), in a p38- and COX-2-dependent manner. Significant concentrations of 15d-PGJ_2 were reached in the medium of melanoma cells, which were sufficient to activate caspase 8 and the mitochondrial pathway of apoptosis. Inhibition of lipocalin-type PGD synthase, a key enzyme for 15d-PGJ_2 synthesis, abolished the apoptotic effect of simvastatin. Moreover, 15d-PGJ_2 was shown to bind to the fatty acid-binding protein 5 (FABP5), which was up-regulated and predominantly detected in the secretome of simvastatin-stressed cells. Knockdown of FABP5 abolished simvastatin-induced activation of PPAR-γ and amplified the apoptotic response.

CONCLUSIONS AND IMPLICATIONS

We characterized simvastatin-induced activation of the 15d-PGJ_2/FABP5 signalling cascades, which triggered an apoptotic burst in melanoma cells but did not affect primary human melanocytes. These data support the rationale for the pharmacological targeting of 15d-PGJ_2 in metastatic melanoma.

Abbreviations

15d-PGJ_2, 15-deoxy-12,14-PGJ_2; FABP5, fatty acid-binding protein 5; FPP, farnesyl pyrophosphate; GGPP, geranylgeranyl pyrophosphate; HMG-CoA, 3-hydroxy-3-methylglutaryl CoA; H-PGDS, haematopoietic PGD synthase; L-PGDS, lipocalin-type PGD synthase; ROS, reactive oxygen species; SDS, sodium dodecyl sulfate

Tables of Links

TARGETS		LIGANDS	
Caspase 3	FABP5	15-deoxy-12,14 PGJ_2	Simvastatin
Caspase 8	H-PGD synthase	Pioglitazone	TNF-α
Caspase 9	L-PGD synthase	Rosiglitazone	TRAIL
COX-2	p38-MAPK	IL-1β	Vincristine
DR5 (TNFRSF10B)	PPAR-γ	SB-203580	

These Tables list key protein targets and ligands in this document, which are hyperlinked to corresponding entries in http://www.guidetopharmacology.org, the common portal for data from the IUPHAR/BPS Guide to PHARMACOLOGY (Pawson *et al.*, 2014) and are permanently archived in the Concise Guide to PHARMACOLOGY 2013/14 (Alexander *et al.*, 2013a,b,c).

Introduction

The 3-hydroxy-3-methylglutaryl-CoA (HMG-CoA) reductase inhibitors (statins) are successfully used to treat hypercholesterolaemia and thereby prevent cardiovascular events (Gazzerro *et al.*, 2012). Over the last decades, the safety profile of statins has shown excellent tolerability in long-term use, with only minor concerns related to drug–drug interactions and genetic polymorphisms involved in alterations of statin pharmacokinetics, leading to liver and skeletal muscle injury (Bellosta and Corsini, 2012; Gazzerro *et al.*, 2012). Other effects than lowering low-density lipoprotein cholesterol have also been reported and are now termed pleiotropic effects (Mihos and Santana, 2011; Gazzerro *et al.*, 2012). On the molecular level, these effects involve cell cycle arrest (Glynn *et al.*, 2008; Saito *et al.*, 2008), induction of apoptosis (Feleszko *et al.*, 2002; Minichsdorfer and Hohenegger, 2009), a reduction in cell migration and inflammation and immunomodulatory effects (Mihos and Santana, 2011). Some of these pleiotropic effects are linked to the depletion of isoprenoids, such as farnesyl pyrophosphate (FPP) and geranylgeranyl pyrophosphate (GGPP) (Collisson *et al.*, 2002; Kidera *et al.*, 2010), which is due to HMG-CoA reductase inhibition. FPP and GGPP are prerequisites for post-translational modification of small G-proteins such as Ras, RhoA and Cdc42. These covalent lipid anchors determine protein localization and hence proper signalling. Statin-induced apoptosis was prevented by co-administration of GGPP in many tumour cell lines, including melanoma cells (Shellman *et al.*, 2005; Saito *et al.*, 2008).

Our laboratory has previously shown that statins induce the mitochondrial pathway of apoptosis in primary human skeletal muscle cells, as well as in human tumour cells, such as rhabdomyosarcoma cells, neuroblastoma cells and metastatic melanoma cell lines A375 and 518a2 (Werner *et al.*, 2004; Sacher *et al.*, 2005; Minichsdorfer and Hohenegger, 2009; Sieczkowski *et al.*, 2010). In metastatic melanoma cells, simvastatin induced an apoptotic burst upon incubation times exceeding 24 h (Minichsdorfer and Hohenegger, 2009). A simple protocol of medium renewal was sufficient to prevent the simvastatin-induced burst of apoptosis. Consequently, an autocrine factor was postulated to be responsible for enhanced activation of caspase 3 via an accessory activation of caspase 8. Fas-ligand is released in murine melanoma cells when treated with a statin (Sarrabayrouse *et al.*, 2007). Nevertheless, the apoptotic burst observed in human metastatic melanoma cells could not be prevented by a neutralizing Fas-ligand antibody (Minichsdorfer and Hohenegger, 2009).

In the light of these findings, such an autocrine factor is of major therapeutic interest. Hence, the objective of our current study was to identify this novel factor that is secreted upon stimulation of human A375 and 518a2 metastatic melanoma cells, which could explain the activation of the extrinsic pathway and the subsequent boost of apoptotic cell death. The specificity of these simvastatin-induced effects was validated by comparing the response of primary human melanocytes with that of primary melanoma cells.

Methods

Cell culture

Primary human melanocytes NHEM (PromoCell, Heidelberg, Germany) and ulli cells (courtesy of Dr Christoph Höller, Department for Dermatology, Medical University Vienna, Austria) were isolated from juvenile foreskin. Primary melanoma cells (6F) were isolated from a melanoma metastasis (courtesy of Dr Christoph Höller) (Schicher *et al.*, 2009). Isolation procedures were approved by the local Ethics Committee of Medical University of Vienna. Primary melanocytes were kept in DermaLife® basal medium supplemented with LifeFactors® (Lifeline, Troisdorf, Germany). The 6F cells (8% fetal calf serum) and human metastatic melanoma cell lines 518a2 and A375 (10% fetal calf serum) were kept in DMEM-high glucose (Invitrogen, Paisley, Scotland, UK) supplemented with 1% penicillin/streptomycin and maintained at 37°C in a 5% CO_2 humidified atmosphere.

Western blot analyses

Following treatments with different agents, cells were lysed in 50 mM Tris–HCl (pH 8.0), 150 mM NaCl, 0.1% SDS, 1% NP-40, 10 mM glycerolphosphate, 1 mM aprotinin, 1 mM leupeptin, 1 mM Pefabloc® (Sigma Chemical Co., St. Louis, MO, USA), 1 mM $NaVO_3$, 5 mM NaF, sonicated and centrifuged (30 000× *g*, 4°C, 40 min). Aliquots of the supernatant (15–30 µg) were separated on SDS polyacrylamide gels and transferred to nitrocellulose membranes for exposure to primary antibodies against COX-2 and lipocalin-type PGD

synthase (L-PGDS) (Cayman Chemical, Hamburg, Germany); p38, phospho-p38, RhoA, Cdc42, cleaved caspases 8, 9 and 3 (Cell Signaling, Frankfurt am Main, Germany); PPAR-γ (Santa Cruz Biotechnology, Heidelberg, Germany); β-actin and α-tubulin (Sigma Chemical Co.); and fatty acid-binding protein 5 (FABP5) (R&D System, Minneapolis, MN, USA). Use of the appropriate HRP-conjugated secondary antibodies enabled specific detection by ECL Plus detection system (GE Healthcare, Bucks, UK). The intensities of the protein bands were measured with Image J software using the gel analysis protocol (http://rsbweb.nih.gov/ij). After background subtraction, the intensities were normalized to the loading control (β-actin or α-tubulin). Alternatively, the ImageQuantTL software (GE Healthcare, Pittsburgh, PA, USA) was used and gave comparable results.

Immunohistochemistry and confocal laser scanning microscopy

Immunohistochemistry was performed as previously described (Werner *et al.*, 2004). Fixed, permeabilized and blocked cells were incubated with primary antibodies against COX-2, FABP5 or PPAR-γ (diluted 1:1000 or 1:500) overnight at 4°C. Thereafter, cells were stained with the corresponding secondary antibodies, anti-mouse-Alexa 488 (1:1000; Invitrogen, Heidelberg, Germany) or anti-rat-Alexa 594 (1:1000; Abcam, Cambridge, UK) for 1 h at room temperature (RT). Nuclei were stained with Hoechst 33342 (1:1000) for 10 min at RT. The mounted slides were analysed on an LSM 510 confocal microscope (Zeiss, Jena, Germany) for fluorescence detection at the appropriate wavelengths using a 63× oil-corrected immersion lens.

15-Deoxy-12,14-PGJ$_2$ (15d-PGJ$_2$) ELISA

The concentration of 15d-PGJ$_2$ was measured with a commercially available ELISA kit (Enzo Life Sciences, Lausen, Switzerland). Briefly, 2×10^5 cells were homogenized in hypotonic buffer (10 mM Tris, 1 mM EDTA, 1 mM aprotinin, 1 mM leupeptin, 1 mM Pefabloc, 1 mM $NaVO_3$; 5 mM NaF), and the cytosolic 15d-PGJ$_2$ concentrations were determined in the supernatant (30 000× *g* at 4°C, 10 min). The corresponding secretion of 15d-PGJ$_2$ was collected from the medium of 2×10^5 cells, acidified (pH 3.5) and applied to a C_{18} reversed-phase extraction column (200 mg 3 mL^{-1}; ChromabondC$_{18}$®, Macherey-Nagel, Düren, Germany). All other steps were performed according to the instruction manual. The cytosolic 15d-PGJ$_2$ was normalized to the protein concentration; secreted 15d-PGJ$_2$ is expressed as pg·mL^{-1}.

Secreted 15d-PGJ$_2$ was also confirmed by reversed-phase HPLC using a C_{18} column (5 µm, 250 × 4.6 mm; Vydac, Grace, IL, USA), 50% acetonitrile/0.1% acetic acid as a mobile phase (2 mL·min^{-1}) and UV detection at 306 nm (Diers *et al.*, 2010). Commercially available 15d-PGJ$_2$ was used as a standard.

Reactive oxygen species (ROS) measurement

The ROS-sensitive fluorescence dye, CellROX® Deep Red Reagent (Invitrogen), was used to detect ROS in aliquots of 1×10^5 melanoma cells incubated for 48 h with the compounds indicated in the figure legend. The resuspended cells were incubated with 5 µM dye for 20 min at 37°C and fixed with 3.7% formaldehyde in 0.9% NaCl. Fluorescence intensity (excitation: 640 nm; emission: 665 nm) was analysed from 10 000 cells on a Becton-Dickinson FACS Calibur (Franklin Lakes, NY, USA) using the Cyflogic software Version 1.2.1 (http://www.cyflogic.com).

JC-1 staining

The mitochondrial membrane potential was monitored by JC-1 (Enzo Life Sciences) accumulation in mitochondria. Melanoma cells (1×10^5) were treated with drugs, as indicated in the figure legends, stained with JC-1 (5 µg·mL^{-1}) for 10 min at 37°C, washed and analysed in the Becton-Dickinson FACScan for aggregates (excitation: 560 nm, emission: 590 nm), monomers (excitation: 488 nm, emission: 529 nm) and the ratio thereof.

Caspase activity measurements

Caspase activity was measured with specific fluorescent caspase 3, 8 and 9 substrates, as previously described (Werner *et al.*, 2004; Minichsdorfer and Hohenegger, 2009; Sieczkowski *et al.*, 2010).

Quantitative real-time PCR and siRNA experiments

The mRNA from 2×10^5 melanoma cells incubated in the absence and presence of 3 µM simvastatin, for 24 or 48 h, was isolated with TriReagent according to manufacturer's instruction. After DNase I treatment, RNA was reverse transcribed using RevertAidH Minus First-Strand cDNA synthesis Kit (Thermo Scientific, Vienna, Austria). Quantitative real-time PCR was performed with SensiMix Plus SYBR & Fluorescein Kit (Bioline, Berlin, Germany) adding cDNA and the specific primer pairs given in Table 1. Four expression controls (GAPDH, B2M, RPLP0, RPS14) were used (Dydensborg *et al.*, 2006). The PCR was run for 40 cycles with 20 s steps for denaturation (95°C), annealing (57°C) and a 25 s elongation step at 72°C followed by a melting curve. C_T values were normalized to the four control genes, and quantification was performed using the comparative C_T method.

FABP5 expression was suppressed by transfection of 2×10^5 melanoma cells with 5 nM siRNA (flexi tube gene solution GS2171) using the HiPerFect® transfection reagent according to the manufacturer's instructions (Qiagen, Hilden, Germany). After 24 h, cells were exposed to 3 µM simvastatin for 48 h and compared with controls.

Two-dimensional difference gel electrophoresis (2D-DIGE) analysis of labelled proteins

The medium (24 mL) of simvastatin- or vincristine-treated 518a2 melanoma cells (48 h) was collected, cleared from cells (1200× *g* for 5 min) and again centrifuged (100 000× *g*, 60 min, 4°C). Proteins in the supernatant were precipitated (ice-cold 6.1 M trichloroacetic acid with 80 mM DTT) and collected by centrifugation (10 000× *g*, 10 min, 4°C) (Zellner *et al.*, 2005; Veitinger *et al.*, 2012). The precipitated proteins were washed with 1.5 mL of ice-cold acetone, including 20 mM DTT, and dry pellets were resuspended in denaturing sample buffer {7 M urea, 2 M thiourea, 4% 3-[(3-cholamidopropyl)dimethylammonio]-1-propanesulfonate and 15 mM Tris–HCl, pH 8.5}. Proteins were labelled with a ratio of 1 µg protein to 5 pmol fluorescent cyanine dyes

Table 1
Specific primer pairs for quantitative PCR experiments

	Primer forward (5′–3′)	Primer reverse (5′–3′)	bp
L-PGDS	CTACTCCGTGTCAGTGGTGG	CACTTATCGGTTTGGGGCAG	213
H-PGDS	AACAAGCTGACTGGCCTGAA	AGTCTGCCCAAGTTACAGAGTT	348
COX-2	ACAGGCTTCCATTGACCAGAG	ATCTGGCCGAGGCTTTTCTAC	208
PPAR-γ	GGGGTTCTCATATCCGAGGG	GGGCGGTCTCCACTGAGAATAA	182
FABP5	ATGAAGGAGCTAGGAGTGGGA	AGCTGTGGTTTCTTCAAACTTCTC	163
Cyclin D1	GCTGCGAAGTGGAAACCATC	GCTCTTTTTCACGGGCTCCA	272
p21	ACTCTCAGGGTCGAAAACGG	AGGAGAACACGGGATGAGGA	366

(CyDyes®, GE Healthcare, Uppsala, Sweden). The secretomes extracted from simvastatin (Cy3)- and vincristine (Cy5)-treated melanoma cells were compared with the negative controls, a secretome of non-stimulated melanoma cells (Cy2). Subsequent isoelectric focusing (30 kVh) and SDS-PAGE were performed as previously described (Veitinger *et al.*, 2012). Spot detection was performed on the gel images using the DeCyder software module Differential In-gel Analysis (version 6.00.28; GE Healthcare) setting the target spot number to 2500. Spots of interest from the separated proteomes were excised from silver-stained gels and digested with trypsin for identification by MS according to the protocol previously provided (Veitinger *et al.*, 2012).

Statistical analysis

The experiments were performed at least three times, carried out in duplicate, and data were presented as mean ± SD, if not otherwise stated. Statistical analysis for multiple comparisons was carried out by one-way ANOVA, followed by *post hoc* Tukey's (Figures 5A, 6, 7, 9, 11 and 13A–C) or Dunnett's test (Figures 3, 5B, 8, 10 and 12) (GraphPad Prism Software, La Jolla, CA, USA). Student's *t*-test was used for statistical analysis of quantitative PCR (Figure 13D). A value of $P < 0.05$ was considered to be statistically significant.

Materials

NS-398 was purchased from Enzo Life Sciences, AT-56 and SC-560 from Tocris Bioscience (Bristol, UK) and 15d-PGJ$_2$ from Santa Cruz Biotechnology. SB-203580, TriReagent, protease inhibitors and all other chemicals were obtained from Sigma Chemical Co. Simvastatin and Mowiol® were purchased from Merck (Rahway, NJ, USA), and the fluorescent substrates for caspases 3, 8 and 9 were from Alexis Biochemicals (San Diego, CA, USA).

Results

Simvastatin induces secretion of a chaperone for lipophilic molecules

Simvastatin (1–10 μM) treatment of human metastatic melanoma cells A375 and 518a2 results in secretion of a suicide factor, which amplified apoptosis by activation of the extrinsic pathway (Minichsdorfer and Hohenegger, 2009). Thus, the proteins in the conditional media were separated by 2D-DIGE to allow identification by MS. In order to control for unspecific protein release due to cytotoxicity, medium from simvastatin (10 μM)-treated 518a2 melanoma cells were compared to vincristine (10 ng·mL^{-1}) exposure. The identified proteins were assigned as cytoskeleton and associated proteins. Introduction of a threshold (regulation greater than fivefold vs. the vincristine positive control and a volume larger than 75 000) scored for three proteins (Figure 1A). Interestingly, two geranylgeranylated Rho GTPases, RhoA and Cdc42, emerged and are clearly related to cytoskeleton interaction and stress fibre formation (Nakata *et al.*, 2006). However, most abundantly up-regulated was the lipid chaperone, FABP5 (Figure 1A and B). FABPs bind hydrophobic ligands with high affinity such as saturated and unsaturated long-chain fatty acids (>C14), eicosanoids and other lipids (Furuhashi and Hotamisligil, 2008).

We confirmed FABP5 up-regulation in A375 and 518a2 melanoma cells by Western blot, immunohistochemistry and on mRNA level (Figures 1C,D and 2C). In order to demonstrate participation of FABP5 in simvastatin-induced apoptosis, the lipid chaperone was down-regulated with siRNA (Figure 1C), but could not prevent simvastatin-induced caspase activation (Figure 1D).

FABP5 recruits eicosanoids to the PPAR-γ, which is known for anti-tumour effects (Michalik *et al.*, 2004; Nunez *et al.*, 2006). On the protein level, PPAR-γ decreased when exposed to simvastatin, which is more pronounced at incubation times of 48 h (Figure 2A). Confocal images also reveal reduced accumulation of PPAR-γ in the nucleus compared with controls (Figure 2C), whereas mRNA levels of PPAR-γ are inconclusive in the presence of simvastatin (Figure 2B). However, quantification of the mRNA of specific PPAR-γ target genes clearly show up-regulation of p21 and down-regulation of cyclin D1 in the presence of simvastatin, which was prevented in FABP5 knockdown cells (Figure 2D). Thus, simvastatin-induced FABP5 is needed to execute PPAR-γ activation, but not to attenuate simvastatin-induced apoptosis (Figure 1E).

Simvastatin-induced apoptosis is dependent upon COX-2 induction and ROS production

The induction of apoptosis by simvastatin is strictly dependent upon HMG-CoA reductase inhibition and is prevented by

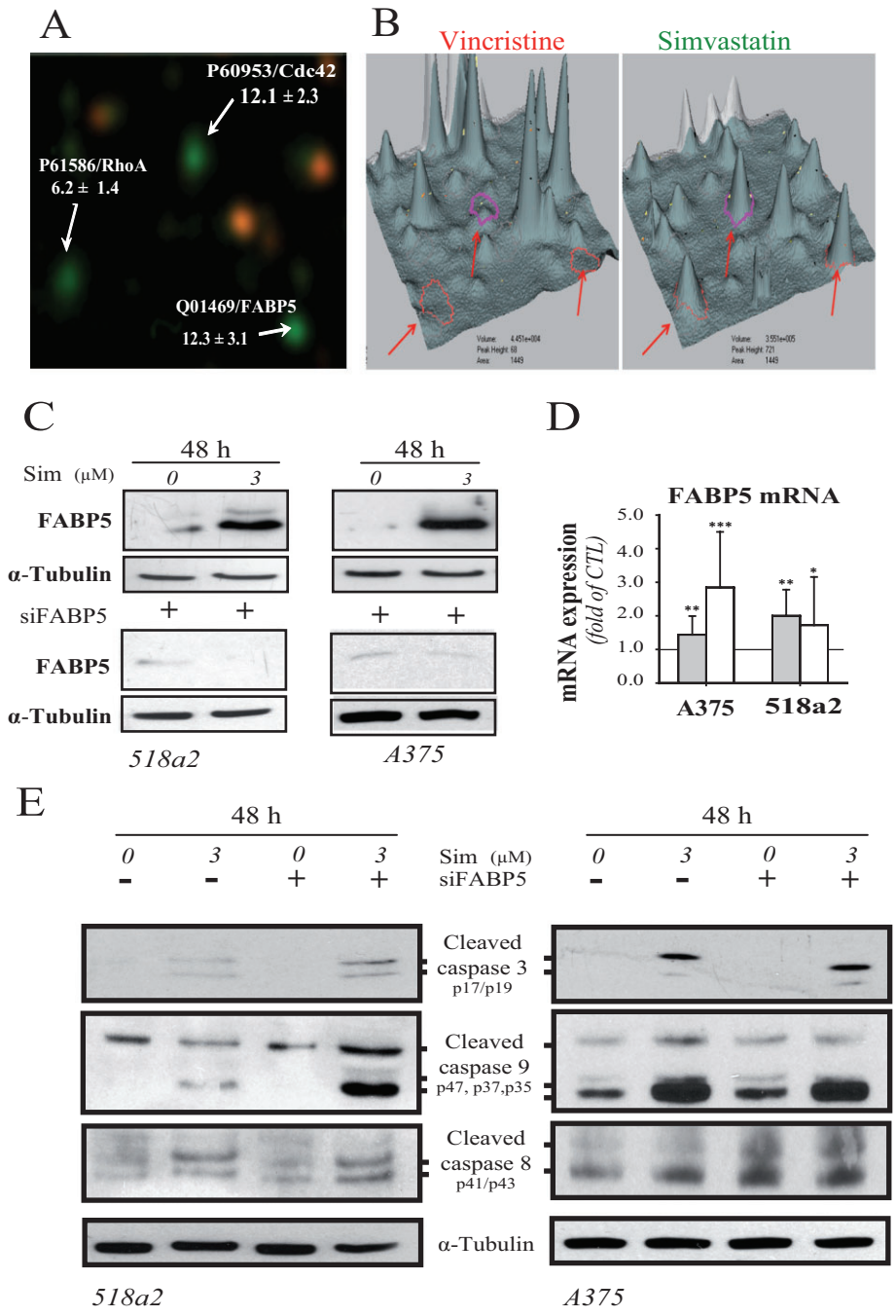

Figure 1

FABP5 expression in metastatic melanoma cells. (A) Analysis of the secretome of 518a2 melanoma cells (by 2D-DIGE) exposed to 10 μM simvastatin (green) or 10 ng·mL^{-1} vincristine (red) for 48 h. A merged picture revealed three proteins of interest, identified by MS (protein identification number). Fold up-regulation is given as mean ± SD (n = 3). Quantification of the proteins of interest (arrows) was confirmed by three-dimensional illustrations (B). Human metastatic melanoma cells, 518a2 and A375, were treated with simvastatin (Sim) for 48 h in the absence and presence of siRNA targeting FABP5 and were analysed for FABP5 protein (C), FABP5 mRNA (D), or cleaved caspase 3, 8 and 9 (E). Quantitative PCR of FABP5 depicts wild-type cells (grey bars) with FABP5 knockdowns (white bars) (n = 3–23). Asterisks indicate significance versus control (*P < 0.05; **P < 0.005; ***P < 0.0005).

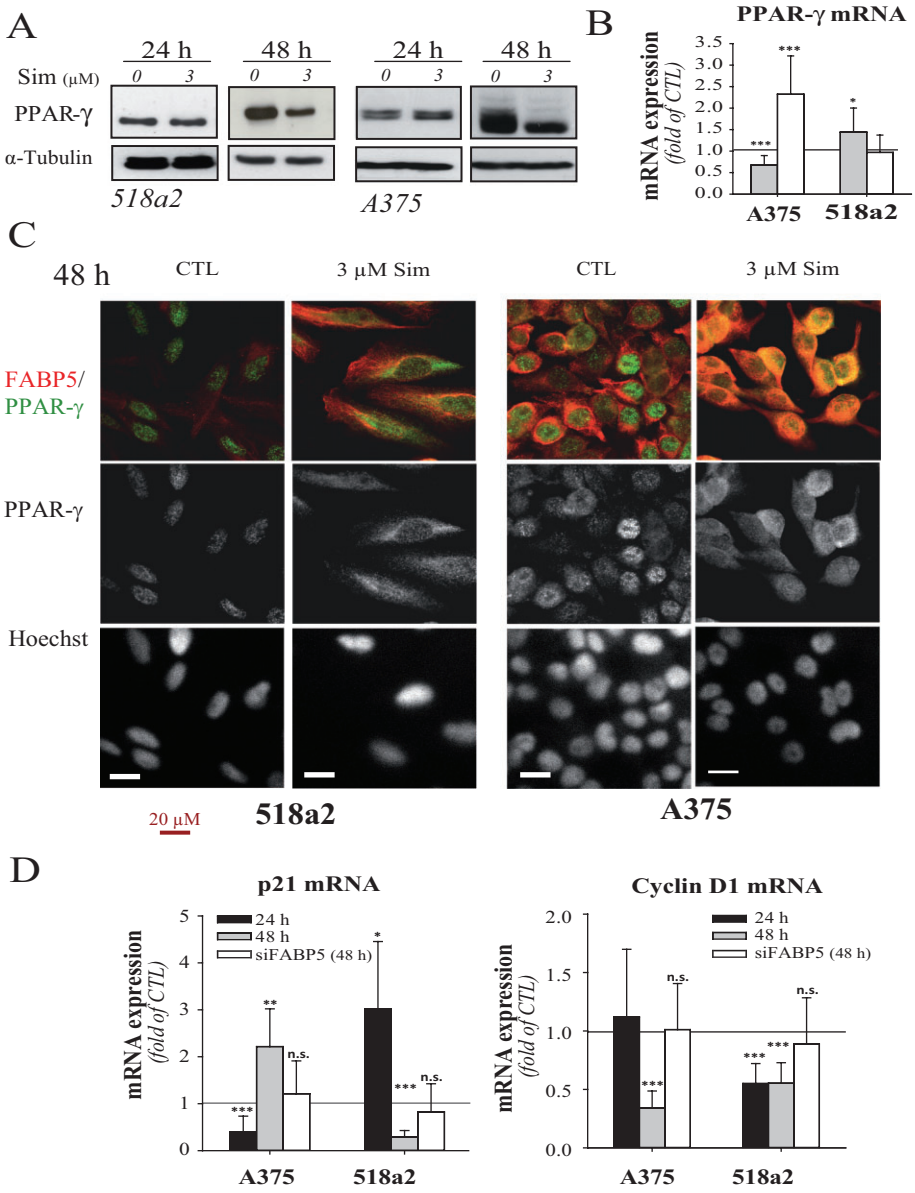

Figure 2

PPAR-γ in simvastatin-treated human melanoma cells. (A) Protein and (B) mRNA levels of PPAR-γ were detected in simvastatin (Sim)-treated metastatic melanoma cells. Analogous to Figure 1D, quantitative PCR for PPAR-γ is illustrated in the absence (grey bars) and presence (white bars) of FABP5 siRNA from simvastatin-treated cells. Similarly, the PPAR-γ targets cyclin D1 and p21 were compared (n = 3–23) (D). (C) PPAR-γ (green) and FABP5 (red) were also visualized in simvastatin-treated cells by confocal microscopy. Nuclei were stained with Hoechst 33342 (grey). Asterisks indicate significance versus control (*P < 0.05; **P < 0.005; ***P < 0.0005; n.s., not significant).

co-administration of mevalonic acid (Minichsdorfer and Hohenegger, 2009). Thus, isoprenylation may be important for RhoA and Cdc42, identified in the secretome of simvastatin-treated melanoma cells (Figure 1). Both GTPases were up-regulated by simvastatin in a concentration- and time-dependent manner (Figure 3). Notably, simvastatin exposure shifted the GTPases to the unprocessed isoform, accompanied by a clear reduction of the processed species (Figure 3A and B). Such an effect on RhoA and Cdc42 may provide sufficient stress signal to activate p38 MAPK. A significant concentration- and time-dependent increase in phosphorylated p38 confirmed this assumption (Figure 3C–E).

The kinase p38 represents a key regulator of inflammation via mediators, including TNF-α, IL-1β and COX-2 (Yano *et al.*, 2007). As we excluded simvastatin-mediated elevation of TNF-α and IL-1β (data not shown), COX-2 expression was further investigated. Simvastatin induced a concentration- and time-dependent induction of COX-2 (Figure 4A). Under resting conditions, COX-2 can be readily detected in 518a2 cells, whereas it is virtually absent in A375 cells, as is evident in confocal microscope images (Figure 4C). COX-2 is strongly induced in A375 cells, as validated by qPCR. In 518a2 cells, such a transcriptional activation of COX-2 was hardly detectable after 24 h (Figure 4B). Importantly, simvastatin-induced

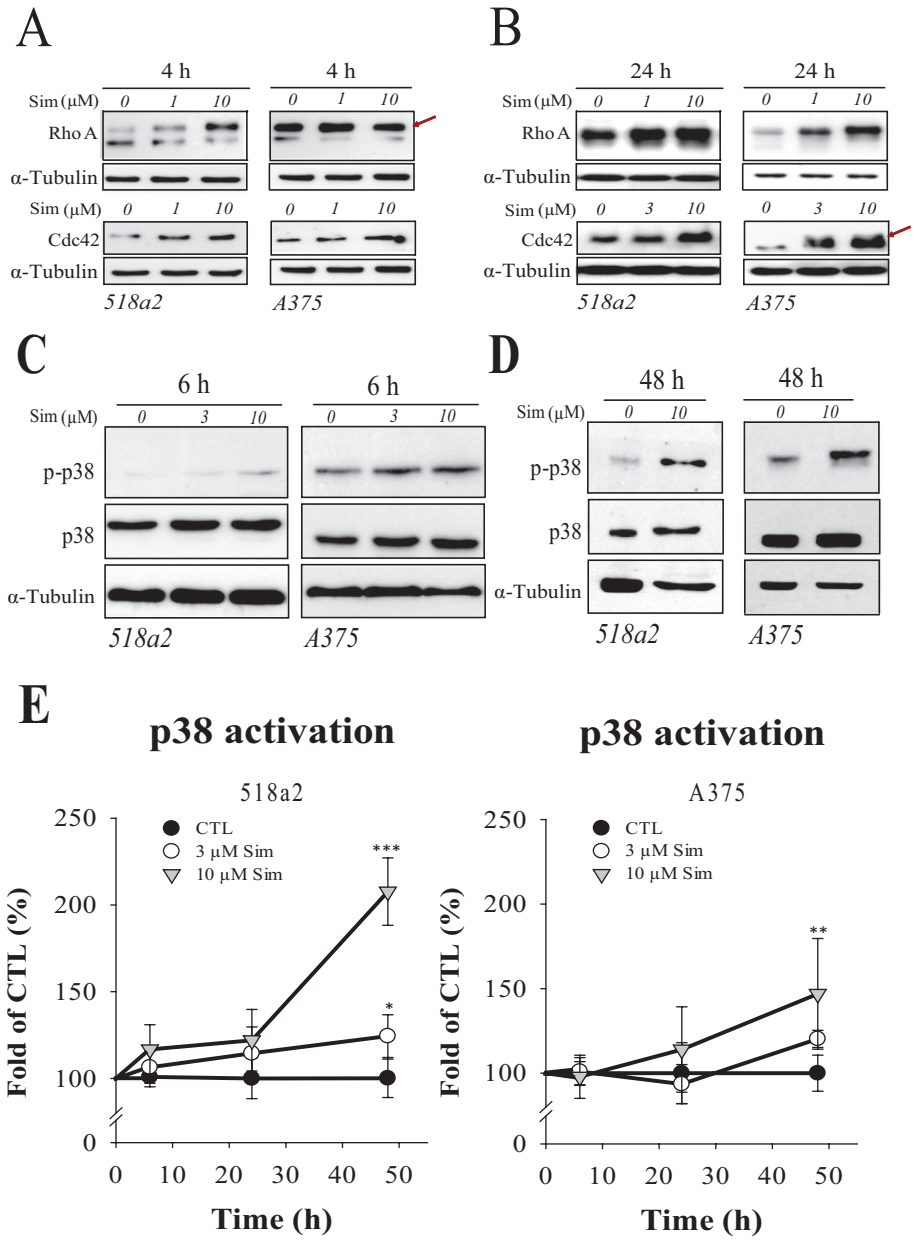

Figure 3

Simvastatin stimulates stress activation via p38. RhoA, Cdc42 and α-tubulin are depicted from cells treated with simvastatin (Sim) for 4 (A) and 24 h (B). The unprocessed forms of the G-proteins are indicated by a red arrow. (C, D) The activation of p38 kinase was monitored by a phospho-specific antibody (p-p38) and compared with total p38 and α-tubulin. (E) Quantification of the p38 phosphorylation is illustrated (n = 3–7). Asterisks indicate significance versus control (*P <0.05; **P < 0.005; ***P < 0.0005).

COX-2 up-regulation was completely abrogated with the specific p38 inhibitor, SB-203580 (Figure 4D). The specific inhibitors for p38 and COX-2, SB-203580 and NS-398, were also used to obtain functional evidence for upstream involvement in simvastatin-induced apoptotic burst. Prototypical concentrations of the inhibitors completely abrogated simvastatin-induced caspase 9 activation (Figure 5A) (Denkert *et al.*, 2001; Yano *et al.*, 2007; Ivanov and Hei, 2011). A concentration of 10 μM NS-398, which is 2.5-fold above the IC_{50} for COX-2 inhibition of the purified enzyme, was not able to significantly reduce simvastatin effects, whereas 50 μM NS-398 did so (Figure 5A) (Futaki *et al.*, 1994). The specific COX-1 inhibitor, SC-560, was not able to abrogate simvastatin-induced caspase 9 activation (Figure 5A), indicating that this isoform is not involved. As caspase 9 activation is preceded by an opening of the mitochondrial transition permeability pore, a breakdown of the mitochondrial membrane potential has to be postulated (Bolisetty and Jaimes, 2013). Indeed, we observed a significant concentration-dependent decline in red JC-1 aggregates (Figure 5B). Mitochondria are the main

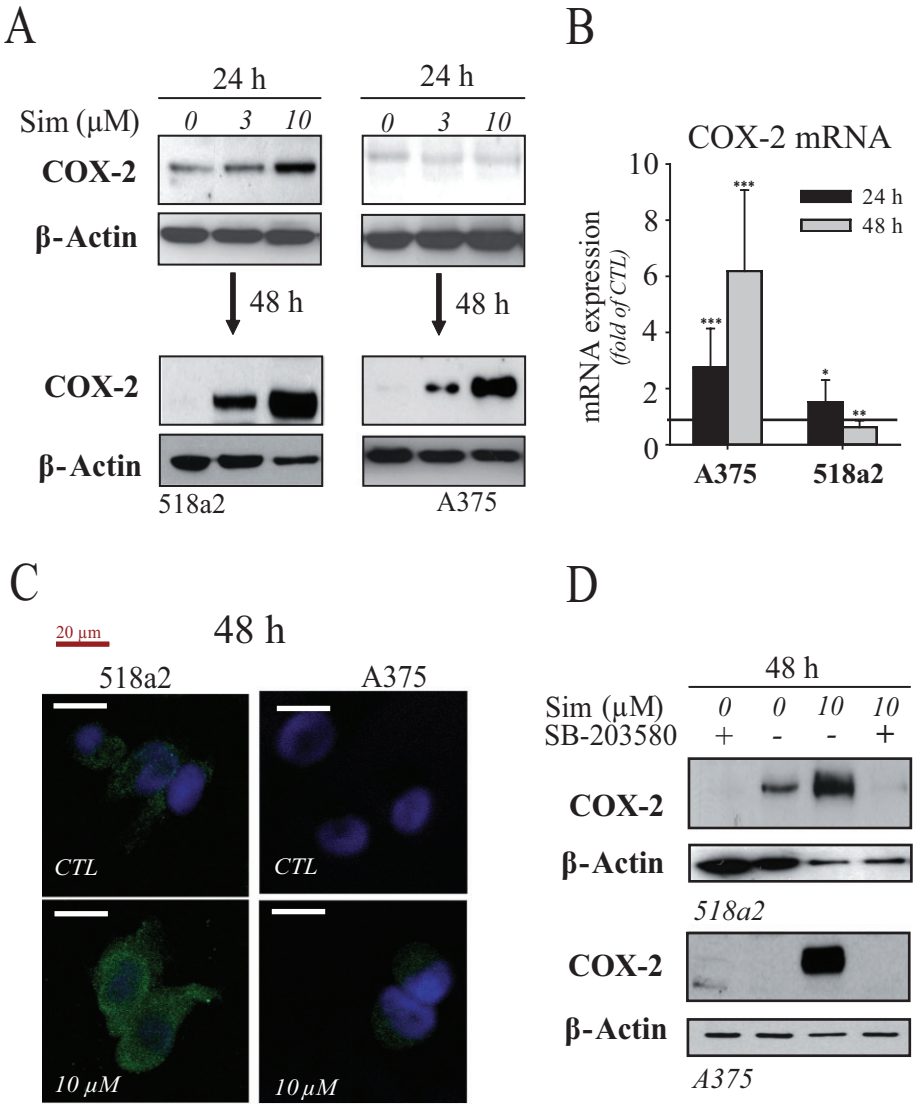

Figure 4

Simvastatin up-regulates COX-2. (A) Simvastatin (Sim)-exposed melanoma cells were probed for protein and (B) mRNA levels of COX-2 (n = 5–10). (C) Confocal fluorescence microscopy images of simvastatin (10 μM)-treated cells revealing enhanced cytosolic COX-2 (green) staining, compared with controls (CTL); nuclei stained with Hoechst 33342 (blue). Representative images are shown. (D) Melanoma cells were exposed to combinations of simvastatin and the p38 inhibitor SB-203580 (10 μM) and analysed for COX-2. Asterisks indicate significance versus control (*P < 0.05; **P < 0.005; ***P < 0.0005).

resource for ROS, under physiological and pathological conditions (Bolisetty and Jaimes, 2013). Simvastatin-induced ROS formation was significantly reduced with *N*-acetylcysteine, which also prevented simvastatin-triggered caspase 9 activation (Figure 6). Most importantly, simvastatin-induced oxidative stress was prevented by co-application of SB-203580 or NS-398, indicating that p38 and COX-2 act upstream of the mitochondrial damage (Figure 7).

15d-PGJ$_2$ is a mediator of simvastatin-induced apoptosis

Thus far, the strong up-regulation of COX-2 (Figure 4) and the considerable protection from simvastatin-induced ROS production by the specific COX-2 inhibitor NS-398 guided us to further consider the role of prostaglandins in this signalling cascade. The prostaglandin 15d-PGJ$_2$ is an endogenous PPAR-γ agonist, recruited and bound to FABP5. Both proteins are regulated by simvastatin. Moreover, 15d-PGJ$_2$ contains a highly reactive cyclopentanone ring, capable of inducing ROS (Kim *et al.*, 2010) in simvastatin-treated metastatic melanoma cells. Simvastatin significantly elevated not only the endogenous synthesis of 15d-PGJ$_2$ but also the secretion of 15d-PGJ$_2$ into the medium up to 95–160 nM (Figure 8). Importantly, secretion of 15d-PGJ$_2$ was inhibited by the specific inhibitors of p38 or COX-2 (Figure 9).

Two prostaglandin D synthases (PGDS) are capable of catalysing the conversion of PGH$_2$ into PGD$_2$ and further to different prostaglandins of the J-series, the lipocalin-type

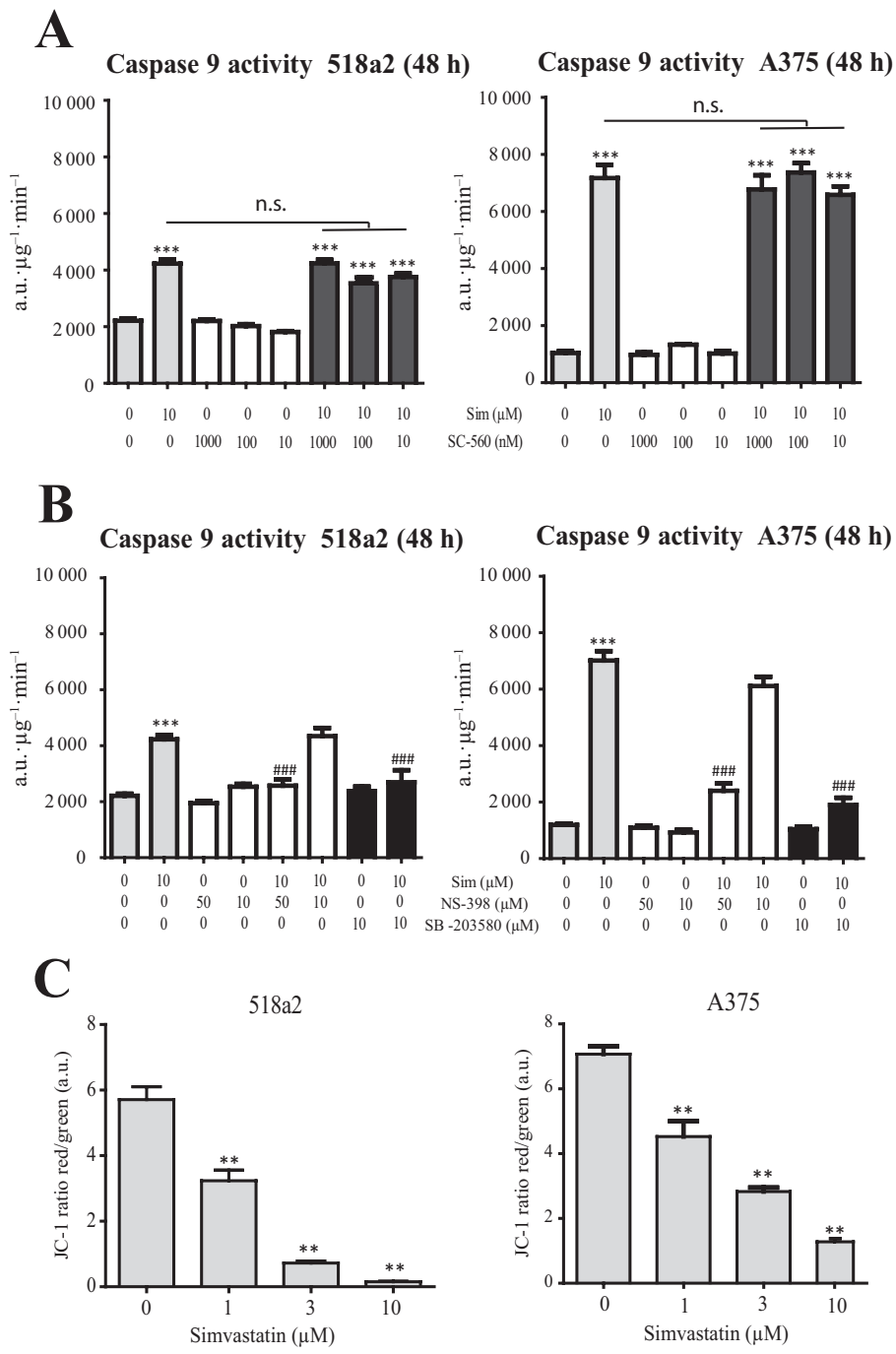

Figure 5

Simvastatin-induced caspase 9 activation is prevented by inhibition of p38 or COX-2, but not COX-1. (A) Metastatic melanoma cells (518a2 and A375) were incubated for 48 h in the absence and presence of simvastatin (Sim) or the specific COX-1 inhibitor SC-560 to measure caspase 9 activation. (B) The specific inhibitors of p38 (SB-203580) and COX-2 (NS-398) inhibited simvastatin (Sim)-triggered caspase 9 activity. Data represent means ± SEM ($n = 3–6$). (C) Cells were stained with JC-1 and analysed by FACS for the ratio of the red/green signal after treatment with simvastatin for 48 h. Data represent the means ± SEM ($n = 8–12$). Asterisks indicate significance versus control (**$P < 0.005$; ***$P < 0.0005$). Hashes indicate significance versus corresponding simvastatin treatment $^{###}P < 0.0005$; n.s., not significant).

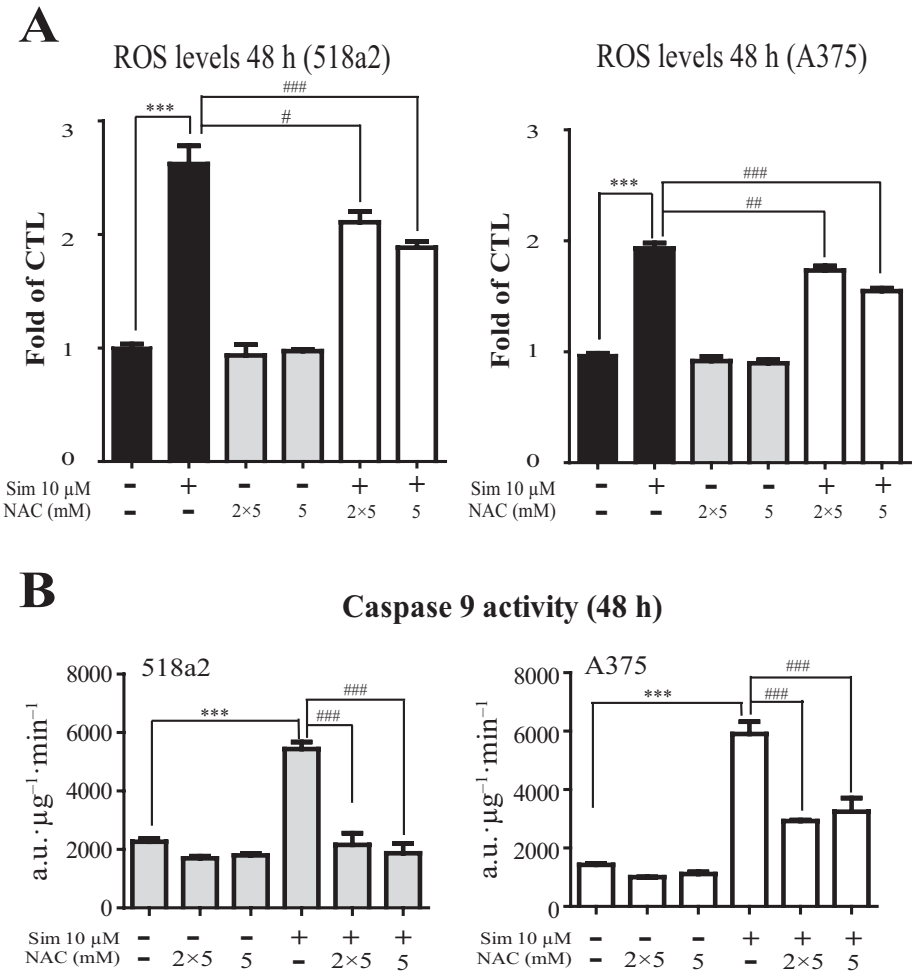

Figure 6

Simvastatin-induced ROS production is associated with caspase 9 activation. (A) The 518a2 and A375 melanoma cells were exposed to simvastatin (Sim) in the absence and presence of 5 µM *N*-acetylcysteine (NAC; 5) or 5 µM NAC every 24 h (2 × 5). After 48 h, ROS formation was detected by FACS. (B) Caspase 9 activity was measured after 48 h in cells treated as given in (A). Bars indicate means ± SEM (n = 3–10). Asterisks indicate significance versus control (***P < 0.0005). Hashes indicate significance versus corresponding simvastatin treatment ($^{\#}P$ < 0.05; $^{\#\#}P$ < 0.005; $^{\#\#\#}P$ < 0.0005; n.s., not significant).

PGDS (L-PGDS) and the hematopoietic PGDS (H-PGDS) (Urade and Eguchi, 2002). On the mRNA level, in A375 melanoma cells, both isoforms were detectable and stimulated by simvastatin (Figure 10). Conversely, in 518a2 cells, we could only detect L-PGDS. On the protein level, the induction of L-PGDS was confirmed in both cell lines.

One may now postulate that inhibition of L-PGDS prevents simvastatin-induced apoptosis, particularly the extrinsic pathway via caspase 8. Indeed, the L-PGDS isoform-specific inhibitor AT-56 prevented the full activation of caspase 9, 8 and, to some extent, caspase 3 (Figure 11).

As an acid test, exogenous 15d-PGJ$_2$ application was sufficient to enhance ROS production and to induce apoptosis via caspase 8 and 9 in metastatic melanoma cells (Figure 12). Similar to the previous observations, ROS formation in 518a2 cells preceded A375 cells (cf. Figure 7). The 15d-PGJ$_2$ was detected in the medium of simvastatin-stressed metastatic melanoma cells lines, but the question remains open whether this holds true also in primary cells. We have therefore investigated primary melanocytes and melanoma 6F cells (Figure 13). Adverse drug events of the skin are very rare in statin-treated humans (Gazzerro *et al.*, 2012). Expectedly, in primary melanocytes, simvastatin was not able to trigger caspase 3 or 15d-PGJ$_2$ formation (Figure 13A and B), in contrast to primary human metastatic melanoma cells (Figure 13C). Moreover, exogenous application of 15d-PGJ$_2$ to 6F cells significantly activated caspase 8 and 9 (Figure 13D) and thereby corroborated our previous finding in metastatic melanoma cell lines.

Taken together, these results corroborate the finding that 15d-PGJ$_2$ acts as a suicide factor in metastatic melanoma cells and simvastatin is the pharmacological trigger for 15d-PGJ$_2$ formation (Figure 14). Thus, one may consider 15d-PGJ$_2$ as a novel lead compound for anti-cancer cyclopentenones.

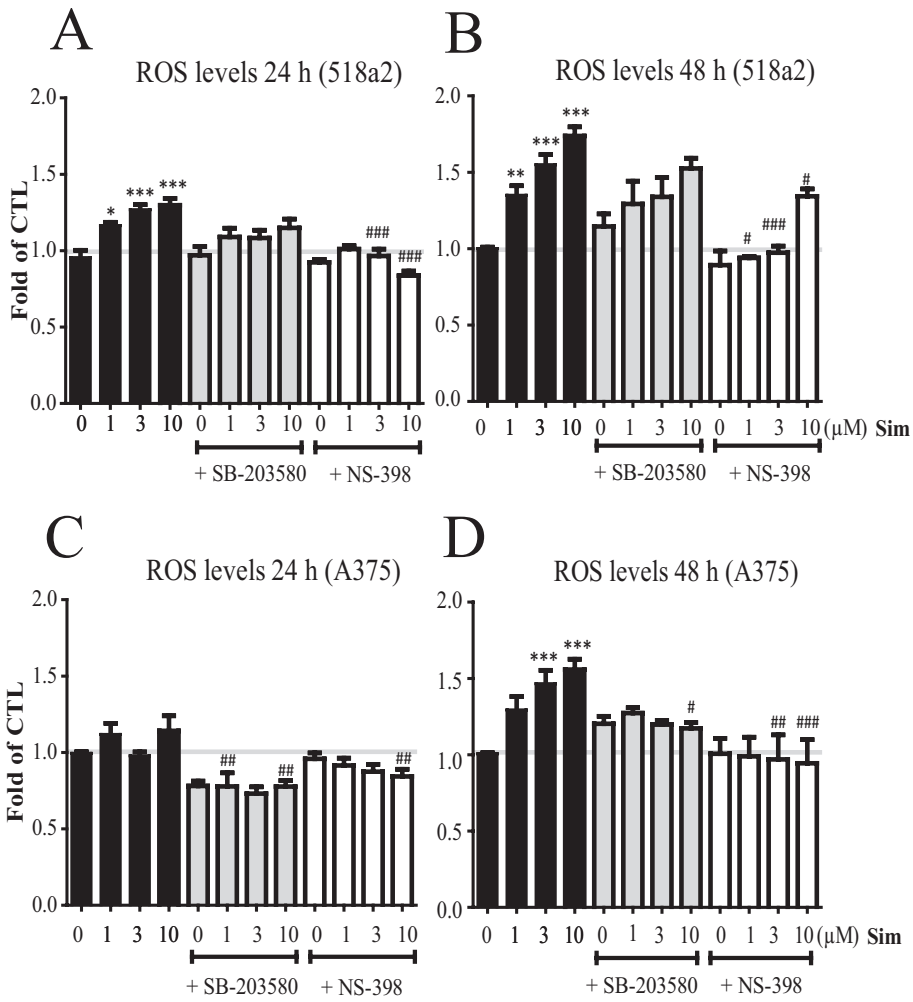

Figure 7

COX-2 and p38 control simvastatin-induced ROS production. The 518a2 (A, B) and A375 (C, D) melanoma cells were exposed to simvastatin (Sim) in the absence and presence of 10 μM SB-203580 or 50 μM NS-398 for 24 (A, C) or 48 h (B, D). Cells were stained for ROS detection by FACS. Data represent the means ± SEM (n = 8–12). Asterisks indicate significance versus control (*P < 0.05; **P < 0.005; ***P < 0.0005). Hashes indicate significance versus corresponding simvastatin treatment ($^{\#}P$ < 0.05; $^{\#\#}P$ < 0.005; $^{\#\#\#}P$ < 0.0005).

Discussion

We here report that the HMG-CoA reductase inhibitor simvastatin is able to elevate intracellular and extracellular prostaglandin 15d-PGJ_2 levels in metastatic melanoma cells (Figure 8) and thereby identify 15d-PGJ_2 as the autocrine suicide factor postulated in our previous work (Minichsdorfer and Hohenegger, 2009). The importance of 15d-PGJ_2 signalling is further corroborated by augmented FABP5 expression in the presence of simvastatin. The lipid chaperone FABP5 binds the lipophilic prostaglandin 15d-PGJ_2 (Coe and Bernlohr, 1998; Furuhashi and Hotamisligil, 2008). FABP5 is abundantly expressed in epidermal cells of the skin and shuttles hydrophobic molecules to different compartments within the cell (Furuhashi and Hotamisligil, 2008). Most importantly, FABP5 transports 15d-PGJ_2 to PPAR-γ (Tan *et al.*, 2002; Ward *et al.*, 2004).

Activation of PPAR-γ leads to anti-cancer effects, cell cycle arrest and pro-apoptotic signalling (Michalik *et al.*, 2004; Nunez *et al.*, 2006). On the protein level, simvastatin reduced PPAR-γ, whereas nuclear translocation of PPAR-γ was not enhanced (Figure 2). However, PPAR-γ ligands 15d-PGJ_2 and FABP5 are strongly up-regulated, which may explain why the two prototypical target genes of PPAR-γ, *cyclin D1* and *p21*, are regulated by simvastatin. *Cyclin D1* down-regulation and *p21* up-regulation (Figure 2D) translate into cell cycle arrest, which has been observed in many statin-treated cancer cell lines, including melanoma cells (Jakobisiak *et al.*, 1991; Glynn *et al.*, 2008; Saito *et al.*, 2008). Importantly, the knockdown of FABP5 abolished the transcriptional activity of PPAR-γ, but not simvastatin-induced activation of caspase 9 and 3 (Figure 1E).

A possible explanation for the detection of FABP5 in the extracellular space is as yet unavailable. However, urinary excretion of FABP5 is described in patients with cutaneous melanoma stage II and III, but not in stage IV melanomas (Brouard *et al.*, 2002). FABP4, a closely related family member, is secreted by adipocytes and circulates in human serum (Xu

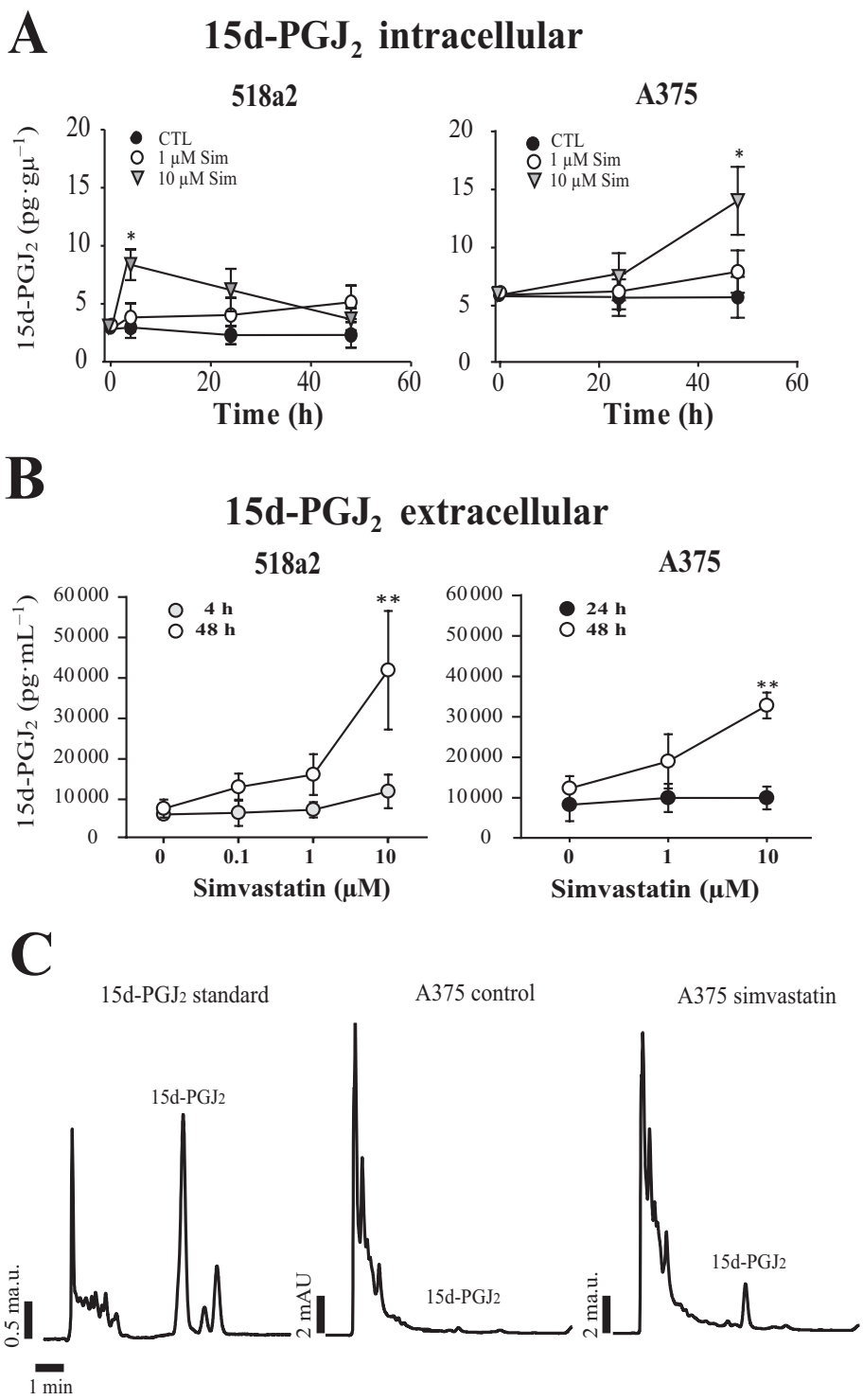

Figure 8

Simvastatin mediates 15d-PGJ$_2$ production. (A) ELISA of 15d-PGJ$_2$ kinetics in the cytosol of simvastatin (Sim)-treated 518a2 or A375 melanoma cells. (B) The extracellular concentration of 15d-PGJ$_2$ in the medium of simvastatin-treated cells is depicted. Data points represent means ± SEM (n = 3–8). (C) HPLC analysis using a 15d-PGJ$_2$ standard (0.3 μg), or 50 μL of the concentrated medium of untreated (control) and simvastatin (10 μM)-treated A375 cells (48 h). Asterisks indicate significance versus control (*P < 0.05; **P < 0.005).

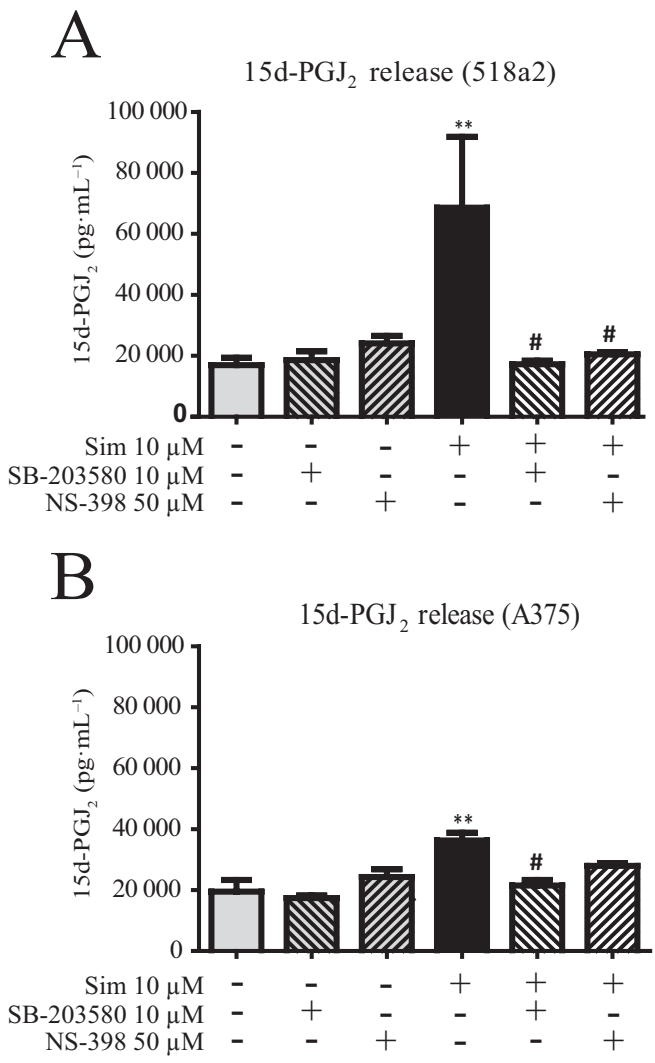

Figure 9

Simvastatin-induced 15d-PGJ_2 secretion is dependent on p38 and COX-2. Human 518a2 (A) and A375 (B) melanoma cells were exposed to simvastatin (Sim), alone or in combination with SB-203580 or NS-398. After 48 h, the extracellular 15d-PGJ_2 concentration was measured. Data represent means ± SEM (n = 3–8). Asterisk indicates significance versus control (**P < 0.005). Hash indicates significance versus corresponding simvastatin treatment ($^{\#}P$ < 0.05).

et al., 2006). Elevated FABP4 serum levels are found in obese individuals and possibly represent a biomarker for metabolic syndrome and obesity (Xu *et al.*, 2006).

Simvastatin-induced apoptosis is clearly controlled by 15d-PGJ_2. This assumption is supported by the following observations. (i) Inhibition of the upstream signal, p38 and COX-2, completely inhibited simvastatin-induced caspase 9 activation, but also the formation of 15d-PGJ_2 (Figures 5 and 9). Basal 15d-PGJ_2 synthesis was not altered by the COX-2 inhibitor NS-398, indicating no cross-reactivity via COX-1. (ii) Simvastatin destroyed already at 1 μM significantly the mitochondrial potential, which is thought to be mediated by ROS formation. However, the inhibitors of p38, COX-2 and the radical scavenger *N*-acetylcysteine protected from this ROS formation (Figures 5–7). (iii) The specific inhibitor of L-PGDS, AT-56, significantly reduced the simvastatin-induced caspase 3 and 9 activity (Figure 11). (iv) Specific activation of caspase 8 is only observed at longer exposure time with simvastatin (Minichsdorfer and Hohenegger, 2009). This apoptotic burst via the extrinsic pathway of apoptosis was also prevented by co-administration with AT-56 (Figure 11). (v) The simvastatin-induced apoptosis and 15d-PGJ_2 formation was not detected in primary human melanocytes, which clearly demonstrates the specificity of these effects. Indirectly, these results are predictable cases of adverse drug reactions are only rarely observed under simvastatin treatment. (vi) Most importantly, even nanomolar concentrations of exogenous 15d-PGJ_2 were sufficient to activate the extrinsic and intrinsic pathways of apoptosis in metastatic melanoma cells.

The multifaceted biological properties of 15d-PGJ_2 include anti-neoplastic, anti-inflammatory and antiviral activities (Surh *et al.*, 2011). Further effects of 15d-PGJ_2, for example, its anti-tumour activity, inhibition of cell cycle progression, induction of heat shock proteins and stimulation of osteogenesis, are observed with statins too (Fukushima, 1992; Surh *et al.*, 2011; Gazzerro *et al.*, 2012). It is worth mentioning that 15d-PGJ_2 has been found to inhibit melanoma progression and tumour stroma interaction (Paulitschke *et al.*, 2012). These effects were independent of PPAR-γ and were not mimicked by other PPAR-γ agonists such as pioglitazone or rosiglitazone. Accordingly, PPAR-γ agonists were not superior to the endogenous ligand 15d-PGJ_2 to prevent tumour proliferation and cell migration in melanoma cells, tumour-associated fibroblasts or tube formation of endothelial cells (Paulitschke *et al.*, 2012). Further evidence for paracrine signalling of 15d-PGJ_2 and anti-tumour activity has been shown in Jurkat T-lymphocytes and prostate cancer cells by induction of death receptor 5 (DR5; also known as TNFRSF10B) and enhanced TRAIL-mediated caspase 8 activity (Nakata *et al.*, 2006). These data indirectly hint towards PPAR-γ-independent signalling of 15d-PGJ_2, which is most likely due to ROS formation and direct interaction with proteins via α,β-unsaturated carbonyl groups located in the cyclopentone ring (Surh *et al.*, 2011). This covalent interaction with proteins then results in cellular stress and ROS formation. Such an assumption is supported by FABP5 knockdown, which amplified apoptosis possibly due to less buffering of 15d-PGJ_2 by the lipid chaperone (Figure 1).

Physiological concentrations of 15d-PGJ_2 are in the pico- to nanomolar concentration range and reach micromolar concentrations at sites of acute inflammation (Fukushima, 1990). In our experiments, 15d-PGJ_2 was confirmed by two independent methods and reached concentrations of 95–160 nM after simvastatin application, which are sixfold higher compared with the media of control cells. Probably higher concentrations can be expected in the microenvironment of melanomas. However, exogenous application of 160 nM 15d-PGJ_2 was sufficient to trigger apoptosis via caspase 8, and ROS formation induced caspase 9 activation (Figures 12 and 13D) in metastatic cell lines and primary melanoma cells.

Statin-induced apoptotic and anti-proliferative effects have been shown in various studies with melanoma cells

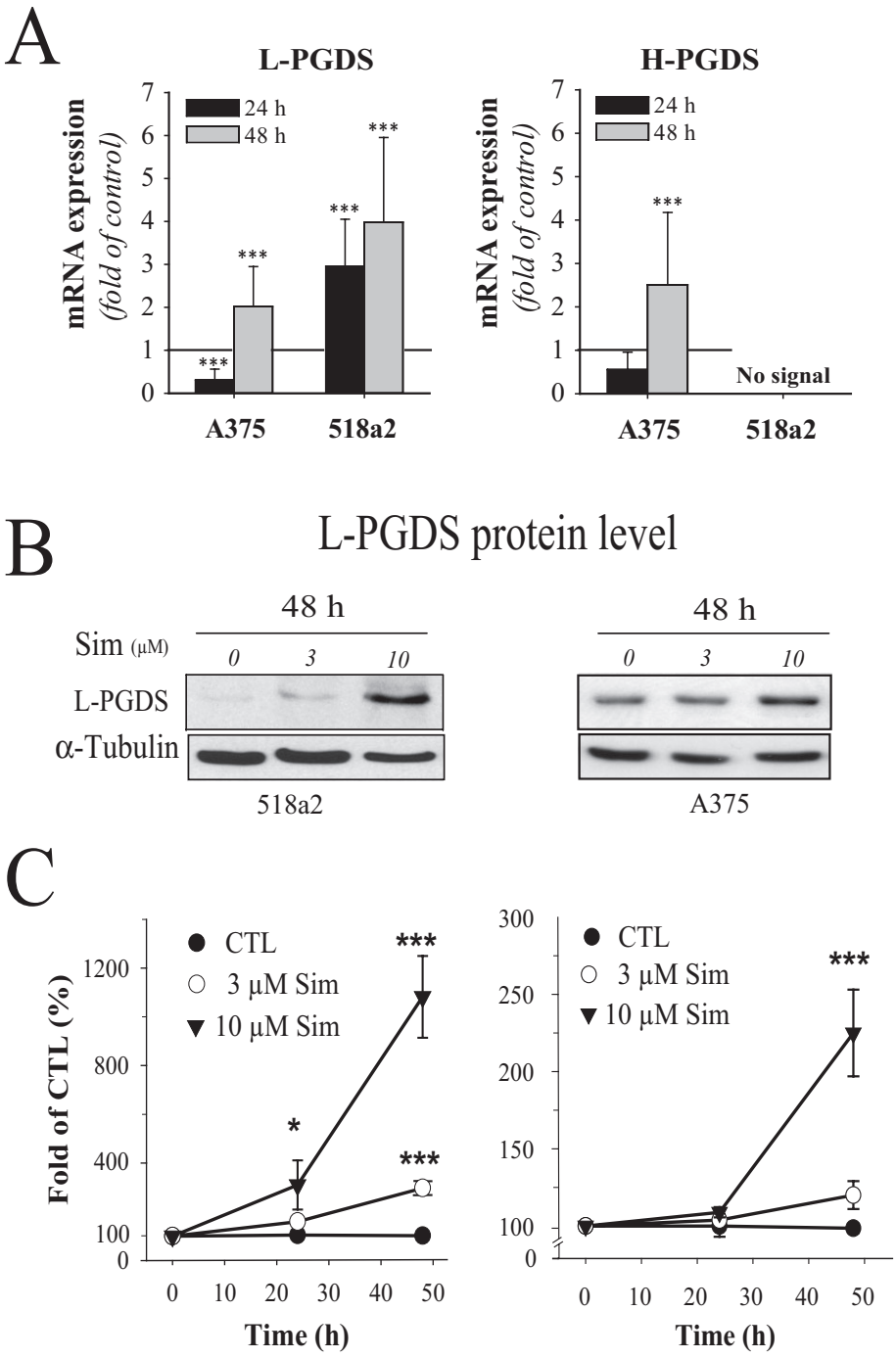

Figure 10

Simvastatin induces PGDS. (A) The mRNA levels of L-PGDS and H-PGDS were determined by quantitative PCR in 518a2 or A375 cells and compared with simvastatin (3 μM, 48 h) treatment (n = 3–12). (B) L-PGDS protein was detected. (C) The kinetics of L-PGDS up-regulation are depicted. Data represent means ± SEM (n = 6). Asterisks indicate significance versus control (*P < 0.05; ***P < 0.0005).

and are affirmed by our study, comparing human A375 and 518a2 metastatic melanoma cells with primary melanocytes and melanoma cells (Dimitroulakos *et al.*, 2001; Shellman *et al.*, 2005; Glynn *et al.*, 2008; Saito *et al.*, 2008). These data are further supported by animal models and xenograft experiments with human and murine melanoma cells. Tumour growth and the metastatic potential was significantly reduced in the statin-treated group (Collisson *et al.*, 2003; Coimbra *et al.*, 2010; Favero *et al.*, 2010; Kidera *et al.*, 2010; Pich *et al.*, 2013). Taken together, there is a large body of evidence suggesting that statins shown to have anti-tumour activity *in vitro* also retain this activity *in vivo*,

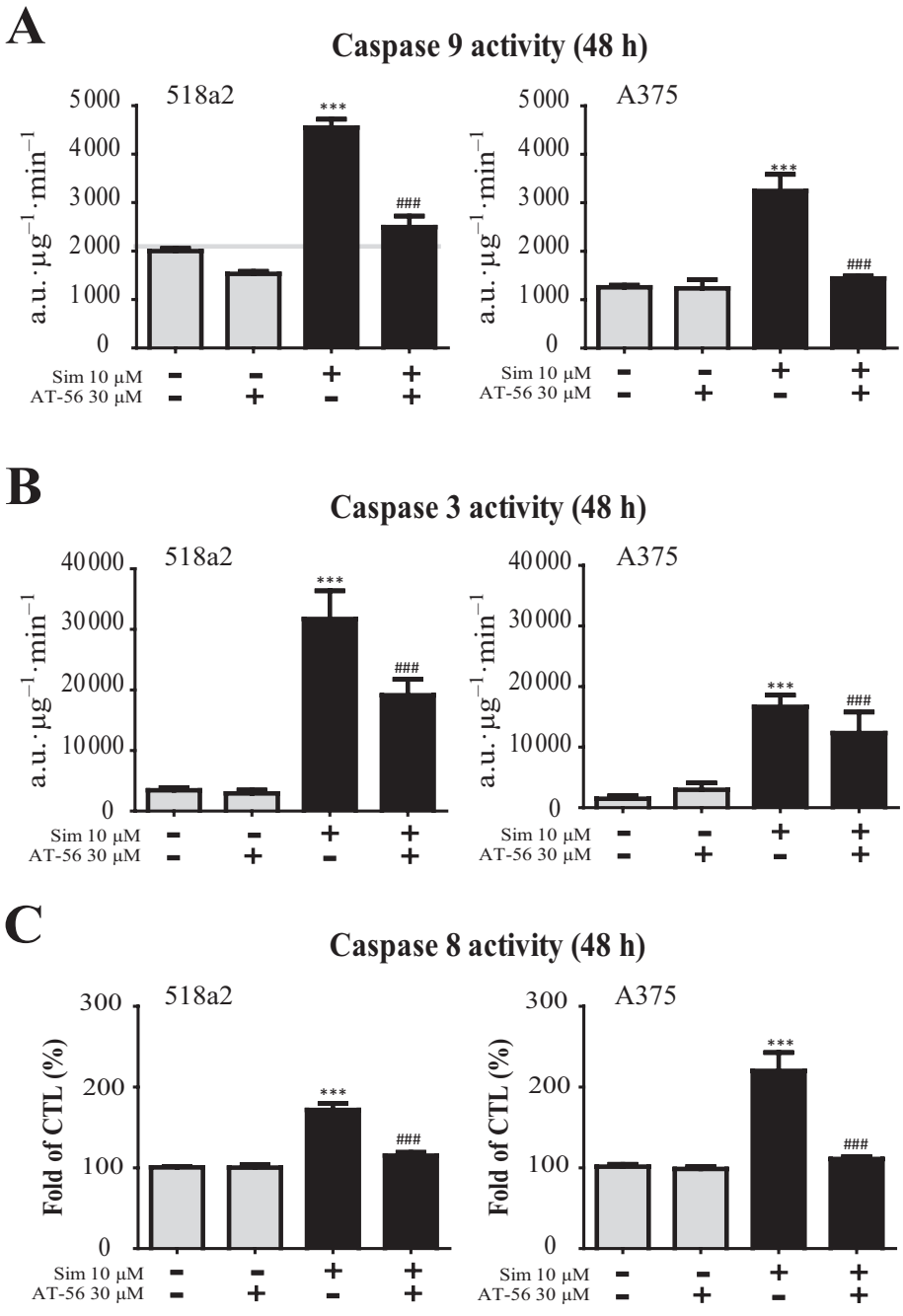

Figure 11

Simvastatin-induced apoptosis is dependent on 15d-PGJ_2. Cells were incubated in the absence and presence of simvastatin (Sim) or the L-PGDS inhibitor AT-56 as indicated. Cell lysates were analysed for caspase 9 (n = 3–8) (A), caspase 3 (n = 3–8) (B) and caspase 8 (n = 4–9) (C) activity. Asterisk indicates significance versus control (***P < 0.0005). Hash indicates significance versus corresponding simvastatin treatment ($^{###}P$ < 0.0005).

which is partially supported in humans. Clinical studies and meta-analyses are available, which confirm a positive outcome and reduced melanoma incidence in statin takers (Koomen *et al.*, 2007; Jacobs *et al.*, 2011; Nielsen *et al.*, 2012). Long-term use of statins revealed an estimated relative risk of the incidence of melanoma of 0.79 (95% CI = 0.66–0.96), similar to endometrial cancer and non-Hodgkin lymphoma (Jacobs *et al.*, 2011). However, some meta-analyses reported no significant evidence for a protective effect on melanoma development, even after subgroup analysis with respect to age, gender, statin type or duration of drug application (Freeman *et al.*, 2006; Bonovas *et al.*, 2010; Jagtap *et al.*, 2012). Nevertheless, a tumour-promoting effect of statins is not observed.

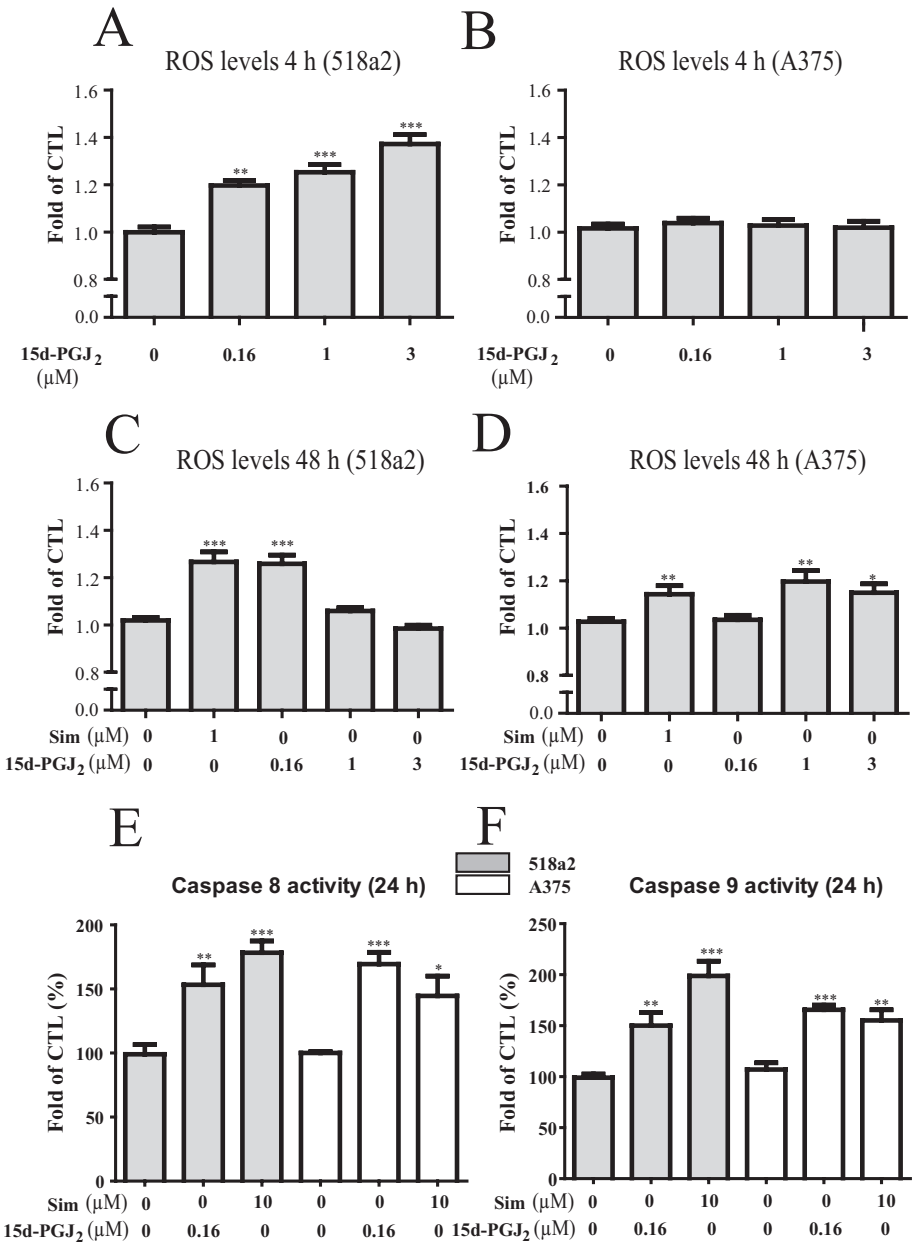

Figure 12

Exogenous 15d-PGJ$_2$ triggers ROS formation and apoptosis. The 518a2 and A375 cells were treated with simvastatin (Sim) or 15d-PGJ$_2$ and ROS formation was analysed after 4 (A, B) and 48 h (C, D). Caspase 8 (E) and caspase 9 (F) are activated by 160 nM 15d-PGJ$_2$, comparable to the effects of simvastatin. Data represent means ± SEM (n = 3–4). Asterisks indicate significance versus control (*P < 0.05; **P < 0.005; ***P < 0.0005).

Although the effects observed with simvastatin were obtained in the concentration range of 1–10 μM, this concentration is over 10–100-fold higher than that used for pharmacological suppression of endogenous cholesterol synthesis (Bellosta and Corsini, 2012). There are reports of clinical trials with higher statin doses, that is, 25 mg lovastatin·kg^{-1}day^{-1}, which resulted in plasma concentrations of 4 μM (Thibault *et al.*, 1996; van der Spek *et al.*, 2006). Similarly, a dose of 15 mg simvastatin·kg^{-1}day^{-1} given for 1 week was well-tolerated and has been investigated in combination with chemotherapeutics in refractory myeloma and lymphoma patients (van der Spek *et al.*, 2006).

In conclusion, simvastatin triggers the synthesis of 15d-PGJ$_2$, a prostaglandin with anti-tumour activity, which explains the apoptotic burst in human metastatic melanoma cells previously observed. These data provide new evidence to support the use of statins in oncological settings and confirm that it is feasible to induce 15d-PGJ$_2$ pharmacologically.

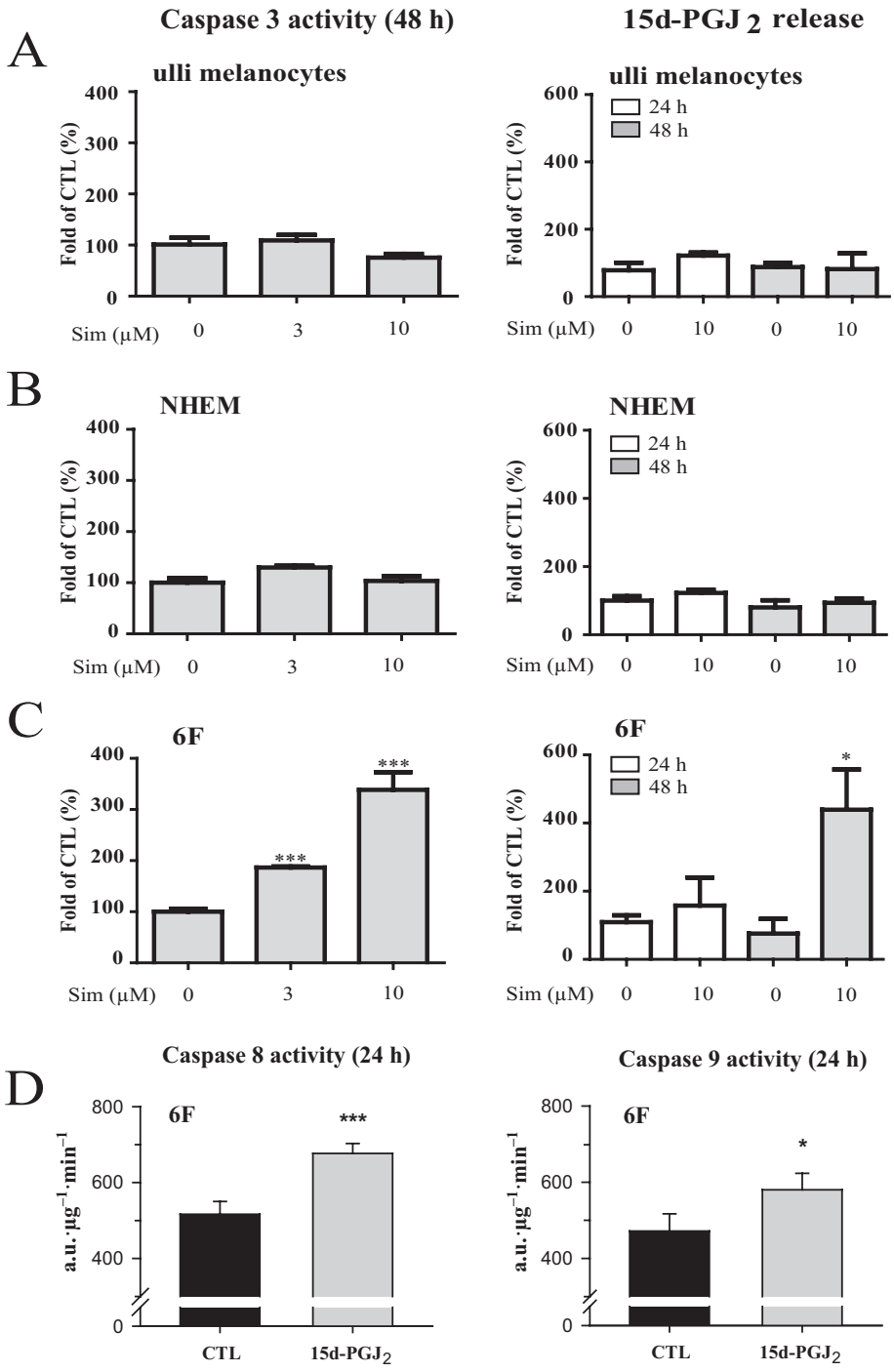

Figure 13

Simvastatin is a trigger for 15d-PGJ_2-induced apoptosis in primary human metastatic melanoma cells but not in melanocytes. Primary human melanocytes, ulli (A) and NHEM (B) and primary human metastatic melanoma cells 6F (C) were incubated with simvastatin for 24 or 48 h in order to measure caspase 3 activity and 15d-PGJ_2 formation ($n = 3$). The 6F cells were also treated in the absence (CTL) and presence of 160 nM 15d-PGJ_2 for 24 h (D) to measure caspase 8 ($n = 4$) and 9 ($n = 3$) activity. Asterisks indicate significance versus control (*$P < 0.05$; ***$P < 0.0005$).

Acknowledgements

This work was supported by Herzfelder'sche Familienstiftung and the Austrian Science Fund (P-22385 to M. H.).

Author contributions

C. W., M. K., C. M., C. H. and M. Z. performed the experiments; C. W., C .H., M. Z. and M. H. contributed to data

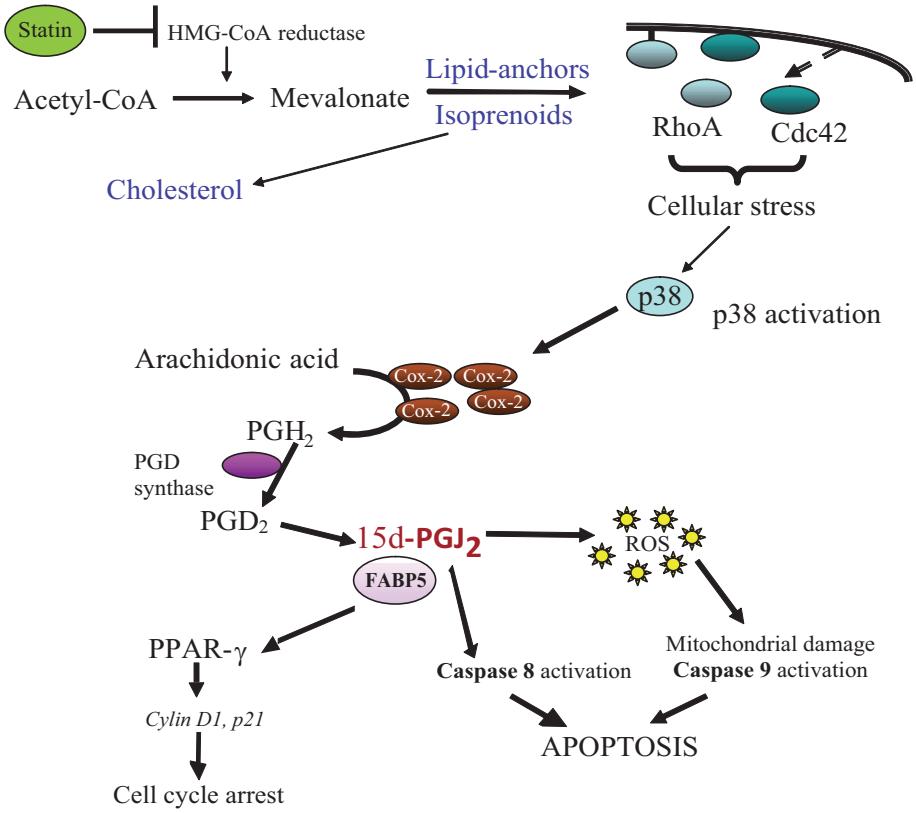

Figure 14
Schematic illustration of 15d-PGJ$_2$ signalling in simvastatin-treated metastatic melanoma cells.

analyses and art work. Design, conception and writing were performed by C. W. and M. H. All authors approved the final version of the manuscript.

Conflict of interest

All authors report no conflict of interest.

References

Alexander SPH, Benson HE, Faccenda E, Pawson AJ, Sharman JL, Spedding M *et al.* (2013a). The Concise Guide to PHARMACOLOGY 2013/14: Nuclear hormone receptors. Br J Pharmacol 170: 1652–1675.

Alexander SPH, Benson HE, Faccenda E, Pawson AJ, Sharman JL, Spedding M *et al.* (2013b). The Concise Guide to PHARMACOLOGY 2013/14: Catalytic receptors. Br J Pharmacol 170: 1676–1705.

Alexander SPH, Benson HE, Faccenda E, Pawson AJ, Sharman JL, Spedding M *et al.* (2013c). The Concise Guide to PHARMACOLOGY 2013/14: Enzymes. Br J Pharmacol 170: 1797–1867.

Bellosta S, Corsini A (2012). Statin drug interactions and related adverse reactions. Expert Opin Drug Saf 11: 933–946.

Bolisetty S, Jaimes EA (2013). Mitochondria and reactive oxygen species: physiology and pathophysiology. Int J Mol Sci 14: 6306–6344.

Bonovas S, Nikolopoulos G, Filioussi K, Peponi E, Bagos P, Sitaras NM (2010). Can statin therapy reduce the risk of melanoma? A meta-analysis of randomized controlled trials. Eur J Epidemiol 25: 29–35.

Brouard MC, Saurat JH, Ghanem G, Siegenthaler G (2002). Urinary excretion of epidermal-type fatty acid-binding protein and S100A7 protein in patients with cutaneous melanoma. Melanoma Res 12: 627–631.

Coe NR, Bernlohr DA (1998). Physiological properties and functions of intracellular fatty acid-binding proteins. Biochim Biophys Acta 1391: 287–306.

Coimbra M, Banciu M, Fens MH, de Smet L, Cabaj M, Metselaar JM *et al.* (2010). Liposomal pravastatin inhibits tumor growth by targeting cancer-related inflammation. J Control Release 148: 303–310.

Collisson EA, Carranza DC, Chen IY, Kolodney MS (2002). Isoprenylation is necessary for the full invasive potential of RhoA overexpression in human melanoma cells. J Invest Dermatol 119: 1172–1176.

Collisson EA, Kleer C, Wu M, De A, Gambhir SS, Merajver SD *et al.* (2003). Atorvastatin prevents RhoC isoprenylation, invasion, and metastasis in human melanoma cells. Mol Cancer Ther 2: 941–948.

Denkert C, Kobel M, Berger S, Siegert A, Leclere A, Trefzer U *et al.* (2001). Expression of cyclooxygenase 2 in human malignant melanoma. Cancer Res 61: 303–308.

Diers AR, Higdon AN, Ricart KC, Johnson MS, Agarwal A, Kalyanaraman B *et al*. (2010). Mitochondrial targeting of the electrophilic lipid 15-deoxy-Delta12,14-prostaglandin J2 increases apoptotic efficacy via redox cell signalling mechanisms. Biochem J 426: 31–41.

Dimitroulakos J, Ye LY, Benzaquen M, Moore MJ, Kamel-Reid S, Freedman MH *et al*. (2001). Differential sensitivity of various pediatric cancers and squamous cell carcinomas to lovastatin-induced apoptosis: therapeutic implications. Clin Cancer Res 7: 158–167.

Dydensborg AB, Herring E, Auclair J, Tremblay E, Beaulieu JF (2006). Normalizing genes for quantitative RT-PCR in differentiating human intestinal epithelial cells and adenocarcinomas of the colon. Am J Physiol Gastrointest Liver Physiol 290: G1067–G1074.

Favero GM, F Otuki M, Oliveira KA, Bohatch MS Jr, Borelli P, Barros FE *et al*. (2010). Simvastatin impairs murine melanoma growth. Lipids Health Dis 9: 142.

Feleszko W, Mlynarczuk I, Olszewska D, Jalili A, Grzela T, Lasek W *et al*. (2002). Lovastatin potentiates antitumor activity of doxorubicin in murine melanoma via an apoptosis-dependent mechanism. Int J Cancer 100: 111–118.

Freeman SR, Drake AL, Heilig LF, Graber M, McNealy K, Schilling LM *et al*. (2006). Statins, fibrates, and melanoma risk: a systematic review and meta-analysis. J Natl Cancer Inst 98: 1538–1546.

Fukushima M (1990). Prostaglandin J2 – anti-tumour and anti-viral activities and the mechanisms involved. Eicosanoids 3: 189–199.

Fukushima M (1992). Biological activities and mechanisms of action of PGJ2 and related compounds: an update. Prostaglandins Leukot Essent Fatty Acids 47: 1–12.

Furuhashi M, Hotamisligil GS (2008). Fatty acid-binding proteins: role in metabolic diseases and potential as drug targets. Nat Rev Drug Discov 7: 489–503.

Futaki N, Takahashi S, Yokoyama M, Arai I, Higuchi S, Otomo S (1994). NS-398, a new anti-inflammatory agent, selectively inhibits prostaglandin G/H synthase/cyclooxygenase (COX-2) activity *in vitro*. Prostaglandins 47: 55–59.

Gazzerro P, Proto MC, Gangemi G, Malfitano AM, Ciaglia E, Pisanti S *et al*. (2012). Pharmacological actions of statins: a critical appraisal in the management of cancer. Pharmacol Rev 64: 102–146.

Glynn SA, O'Sullivan D, Eustace AJ, Clynes M, O'Donovan N (2008). The 3-hydroxy-3-methylglutaryl-coenzyme A reductase inhibitors, simvastatin, lovastatin and mevastatin inhibit proliferation and invasion of melanoma cells. BMC Cancer 8: 9.

Ivanov VN, Hei TK (2011). Regulation of apoptosis in human melanoma and neuroblastoma cells by statins, sodium arsenite and TRAIL: a role of combined treatment versus monotherapy. Apoptosis 16: 1268–1284.

Jacobs EJ, Newton CC, Thun MJ, Gapstur SM (2011). Long-term use of cholesterol-lowering drugs and cancer incidence in a large United States cohort. Cancer Res 71: 1763–1771.

Jagtap D, Rosenberg CA, Martin LW, Pettinger M, Khandekar J, Lane D *et al*. (2012). Prospective analysis of association between use of statins and melanoma risk in the Women's Health Initiative. Cancer 118: 5124–5131.

Jakobisiak M, Bruno S, Skierski JS, Darzynkiewicz Z (1991). Cell cycle-specific effects of lovastatin. Proc Natl Acad Sci U S A 88: 3628–3632.

Kidera Y, Tsubaki M, Yamazoe Y, Shoji K, Nakamura H, Ogaki M *et al*. (2010). Reduction of lung metastasis, cell invasion, and adhesion in mouse melanoma by statin-induced blockade of the Rho/Rho-associated coiled-coil-containing protein kinase pathway. J Exp Clin Cancer Res 29: 127.

Kim DH, Kim EH, Na HK, Sun Y, Surh YJ (2010). 15-Deoxy-Delta(12,14)-prostaglandin J(2) stabilizes, but functionally inactivates p53 by binding to the cysteine 277 residue. Oncogene 29: 2560–2576.

Koomen ER, Joosse A, Herings RM, Casparie MK, Bergman W, Nijsten T *et al*. (2007). Is statin use associated with a reduced incidence, a reduced Breslow thickness or delayed metastasis of melanoma of the skin? Eur J Cancer 43: 2580–2589.

Michalik L, Desvergne B, Wahli W (2004). Peroxisome-proliferator-activated receptors and cancers: complex stories. Nat Rev Cancer 4: 61–70.

Mihos CG, Santana O (2011). Pleiotropic effects of the HMG-CoA reductase inhibitors. Int J Gen Med 4: 261–271.

Minichsdorfer C, Hohenegger M (2009). Autocrine amplification loop in statin-induced apoptosis of human melanoma cells. Br J Pharmacol 157: 1278–1290.

Nakata S, Yoshida T, Shiraishi T, Horinaka M, Kouhara J, Wakada M *et al*. (2006). 15-Deoxy-Delta12,14-prostaglandin J(2) induces death receptor 5 expression through mRNA stabilization independently of PPARgamma and potentiates TRAIL-induced apoptosis. Mol Cancer Ther 5: 1827–1835.

Nielsen SF, Nordestgaard BG, Bojesen SE (2012). Statin use and reduced cancer-related mortality. N Engl J Med 367: 1792–1802.

Nunez NP, Liu H, Meadows GG (2006). PPAR-gamma ligands and amino acid deprivation promote apoptosis of melanoma, prostate, and breast cancer cells. Cancer Lett 236: 133–141.

Paulitschke V, Gruber S, Hofstatter E, Haudek-Prinz V, Klepeisz P, Schicher N *et al*. (2012). Proteome analysis identified the PPARgamma ligand 15d-PGJ2 as a novel drug inhibiting melanoma progression and interfering with tumor-stroma interaction. PLoS ONE 7: e46103.

Pich C, Teiti I, Rochaix P, Mariame B, Couderc B, Favre G *et al*. (2013). Statins reduce melanoma development and metastasis through MICA overexpression. Front Immunol 4: 62.

Sacher J, Weigl L, Werner M, Szegedi C, Hohenegger M (2005). Delineation of myotoxicity induced by 3-hydroxy-3-methylglutaryl CoA reductase inhibitors in human skeletal muscle cells. J Pharmacol Exp Ther 314: 1032–1041.

Saito A, Saito N, Mol W, Furukawa H, Tsutsumida A, Oyama A *et al*. (2008). Simvastatin inhibits growth via apoptosis and the induction of cell cycle arrest in human melanoma cells. Melanoma Res 18: 85–94.

Sarrabayrouse G, Synaeve C, Leveque K, Favre G, Tilkin-Mariame AF (2007). Statins stimulate *in vitro* membrane FasL expression and lymphocyte apoptosis through RhoA/ROCK pathway in murine melanoma cells. Neoplasia 9: 1078–1090.

Schicher N, Paulitschke V, Swoboda A, Kunstfeld R, Loewe R, Pilarski P *et al*. (2009). Erlotinib and bevacizumab have synergistic activity against melanoma. Clin Cancer Res 15: 3495–3502.

Shellman YG, Ribble D, Miller L, Gendall J, Vanbuskirk K, Kelly D *et al*. (2005). Lovastatin-induced apoptosis in human melanoma cell lines. Melanoma Res 15: 83–89.

Sieczkowski E, Lehner C, Ambros PF, Hohenegger M (2010). Double impact on p-glycoprotein by statins enhances doxorubicin cytotoxicity in human neuroblastoma cells. Int J Cancer 126: 2025–2035.

van der Spek E, Bloem AC, van de Donk NW, Bogers LH, van der Griend R, Kramer MH *et al*. (2006). Dose-finding study of high-dose simvastatin combined with standard chemotherapy in patients with relapsed or refractory myeloma or lymphoma. Haematologica 91: 542–545.

Pawson AJ, Sharman JL, Benson HE, Faccenda E, Alexander SP, Buneman OP *et al*.; NC-IUPHAR (2014). The IUPHAR/BPS Guide to PHARMACOLOGY: an expert-driven knowledgebase of drug targets and their ligands. Nucl. Acids Res. 42 (Database Issue): D1098–106.

Surh YJ, Na HK, Park JM, Lee HN, Kim W, Yoon IS *et al*. (2011). 15-Deoxy-Delta(1)(2),(1)(4)-prostaglandin J(2), an electrophilic lipid mediator of anti-inflammatory and pro-resolving signaling. Biochem Pharmacol 82: 1335–1351.

Tan NS, Shaw NS, Vinckenbosch N, Liu P, Yasmin R, Desvergne B *et al*. (2002). Selective cooperation between fatty acid binding proteins and peroxisome proliferator-activated receptors in regulating transcription. Mol Cell Biol 22: 5114–5127.

Thibault A, Samid D, Tompkins AC, Figg WD, Cooper MR, Hohl RJ *et al*. (1996). Phase I study of lovastatin, an inhibitor of the mevalonate pathway, in patients with cancer. Clin Cancer Res 2: 483–491.

Urade Y, Eguchi N (2002). Lipocalin-type and hematopoietic prostaglandin D synthases as a novel example of functional convergence. Prostaglandins Other Lipid Mediat 68–69: 375–382.

Veitinger M, Umlauf E, Baumgartner R, Badrnya S, Porter J, Lamont J *et al*. (2012). A combined proteomic and genetic analysis of the highly variable platelet proteome: from plasmatic proteins and SNPs. J Proteomics 75: 5848–5860.

Ward JE, Gould H, Harris T, Bonacci JV, Stewart AG (2004). PPAR gamma ligands, 15-deoxy-delta12,14-prostaglandin J2 and rosiglitazone regulate human cultured airway smooth muscle proliferation through different mechanisms. Br J Pharmacol 141: 517–525.

Werner M, Sacher J, Hohenegger M (2004). Mutual amplification of apoptosis by statin-induced mitochondrial stress and doxorubicin toxicity in human rhabdomyosarcoma cells. Br J Pharmacol 143: 715–724.

Xu A, Wang Y, Xu JY, Stejskal D, Tam S, Zhang J *et al*. (2006). Adipocyte fatty acid-binding protein is a plasma biomarker closely associated with obesity and metabolic syndrome. Clin Chem 52: 405–413.

Yano M, Matsumura T, Senokuchi T, Ishii N, Murata Y, Taketa K *et al*. (2007). Statins activate peroxisome proliferator-activated receptor gamma through extracellular signal-regulated kinase 1/2 and p38 mitogen-activated protein kinase-dependent cyclooxygenase-2 expression in macrophages. Circ Res 100: 1442–1451.

Zellner M, Winkler W, Hayden H, Diestinger M, Eliasen M, Gesslbauer B *et al*. (2005). Quantitative validation of different protein precipitation methods in proteome analysis of blood platelets. Electrophoresis 26: 2481–2489.